

# Exact potentials in multivariate Langevin equations

Tiemo Pedergnana<sup>1</sup> and Nicolas Noiray<sup>1</sup>

CAPS Laboratory, Department of Mechanical and Process Engineering, ETH Zürich, Sonneggstrasse 3, 8092 Zürich, Switzerland

(\*Electronic mail: noirayn@ethz.ch)

(\*Electronic mail: ptiamo@ethz.ch)

(Dated: October 25, 2022)

Systems governed by a multivariate Langevin equation featuring an exact potential exhibit straightforward dynamics but are often difficult to recognize because, after a general coordinate change, the gradient flow becomes obscured by the Jacobian matrix of the mapping. In this work, a detailed analysis of the transformation properties of Langevin equations under general nonlinear mappings is presented. We show how to identify systems with exact potentials by understanding their differential-geometric properties. To demonstrate the power of our method, we use it to derive exact potentials for broadly studied models of nonlinear deterministic and stochastic oscillations. In selected examples, we visualize the potentials to illustrate how our method enables new analytical descriptions of the classic phenomena of beating, synchronization and symmetry breaking. Our results imply a broad class of exactly solvable stochastic models which can be self-consistently defined from given deterministic gradient systems.

**Since the seminal works of Albert Einstein and Paul Langevin on Brownian motion, the study of stochastic dynamics has developed into a fruitful science which today finds application in many fields. For an important subclass of noise-driven systems, those governed by a Langevin equation with an exact stationary potential, the steady-state dynamics may be solved analytically. Despite the great benefits of these solutions, the subtleties of identifying exact potentials in systems which are described in transformed variables have apparently been ignored so far. To fill this gap in the literature, we derive the differential-geometric transformation properties of multivariate Langevin equations under general coordinate changes and we demonstrate how they can lead to new analytical descriptions of a system's nonlinear dynamics. The method is then applied to different examples of deterministic and noise-driven oscillations, yielding analytical descriptions of important physical phenomena such as beating, synchronization and symmetry breaking. Finally, we comment on a broad class of exactly solvable models implied by our results, which enable self-consistent and analytical modeling of additive noise in given deterministic gradient flows.**

## I. INTRODUCTION

In systems featuring exact potentials, the evolution of a  $n$ -dimensional set of variables  $x = (x_1, \dots, x_n)^T: \mathbb{R} \rightarrow \mathbb{R}^n$  over time  $t \in \mathbb{R}$  is governed by the Langevin equation with potential (LP)<sup>1,2</sup>

$$\dot{x} = -\nabla \mathcal{V}(x, t) + \Xi, \quad (1)$$

where  $\nabla_i = \partial/\partial x_i$ ,  $\mathcal{V}: \mathbb{R}^n \rightarrow \mathbb{R}$  is the potential,  $\mathcal{F}_i = -\nabla_i \mathcal{V}(x, t)$  is the  $i$ th component of the restoring force  $\mathcal{F}$  and the vector  $\Xi = (\xi_1, \dots, \xi_n)^T: \mathbb{R} \rightarrow \mathbb{R}^n$  contains uncorrelated white noise sources  $\xi_i$ ,  $i = 1, \dots, n$  of equal intensity  $\Gamma$ . The individual entries  $\xi_i$  of  $\Xi$  are assumed to be delta-correlated:

$\langle \xi_i \xi_j(\tau) \rangle = \Gamma \delta_{ij} \delta(\tau)$ , where  $\langle \cdot \rangle$  is the expected value operator,  $(\cdot)_{,\tau}$  denotes a positive time shift by  $\tau$  and  $\delta$  is the Dirac delta function.<sup>3</sup>

The modern study of Langevin equations dates back over a century,<sup>4</sup> and they continue to be an active topic of research today.<sup>5–9</sup> Well known, low-dimensional examples of LPs are the Stuart–Landau oscillator<sup>10–12</sup> subject to additive noise, whose deterministic part represents the normal form of a supercritical Hopf bifurcation,<sup>13</sup> (p. 270) and the deterministically and stochastically averaged noise-driven Van der Pol oscillator.<sup>3,14–17</sup> As will be discussed in the present work, multivariate systems governed by potentials are also found in the classic Kuramoto model,<sup>18,19</sup> swarming oscillators,<sup>20</sup> classical many-body time crystals,<sup>21</sup> networks of coupled limit cycles<sup>17,22,23</sup> and in models of noise-driven, self-sustained thermoacoustic modes of annular cavities.<sup>24–27</sup> We mention that exact potentials occur also in models of turbulent wakes,<sup>28</sup> swirling flows<sup>29</sup> and buoyancy-driven bodies.<sup>30</sup>

This work deals with noise-driven systems in the form of ordinary stochastic differential equations. The reader interested in applications of exact potentials in partial differential equations is referred to the relevant literature.<sup>31–35</sup>

In general, multivariate dynamical systems do not possess an exact potential. While the problem of finding meaningful quasi-potentials in systems that are *not* governed by an exact potential has been tackled in the past,<sup>36,37</sup> there are also many relevant multivariate systems subject to random noise *with* exact potentials. If one exists, knowing the exact potential is a great benefit because it fully determines the stochastic dynamics in the steady state. The problem practitioners face is that it is often difficult to perceive the existence of a potential when the system is described with transformed variables. This issue is addressed in this work.

In particular, we are concerned with identifying the presence of an underlying exact potential in general noise-driven systems taking the form

$$\dot{x} = \mathcal{F}(x, t) + \mathcal{B}(x)\Xi, \quad (2)$$

where  $\mathcal{F}$  is a vector- and  $\mathcal{B}$  a  $n$ -by- $n$  tensor field.<sup>1</sup> With the

knowledge of  $\mathcal{F}$ , assuming a LP (1), one can easily deduce if an exact potential  $\mathcal{V}$  exists for  $x$  by checking the following necessary and sufficient conditions<sup>2</sup> (pp. 133–134):

$$\nabla_i \mathcal{F}_j = \nabla_j \mathcal{F}_i \quad (3)$$

for all  $i$  and  $j \neq i$ . However, if these conditions are not fulfilled, this does not preclude the existence of an exact potential governing the original variables that were transformed into  $x$  via a certain nonlinear mapping. We therefore argue that, instead of applying Eq. (3), Eq. (2) should be compared to a LP after a coordinate change defined by an arbitrary nonlinear mapping

$$x = f(y), \quad (4)$$

see Fig. 1. Assuming purely additive noise in the equations governing the underlying potential system which transforms objectively under local rotations and reflections, the resulting transformed Langevin equation with potential (TLP) reads, after redefining  $y \rightarrow x$ ,

$$\dot{x} = -g^{-1}(x) \nabla \tilde{\mathcal{V}}(x, t) + h^{-1}(x) \Xi, \quad (5)$$

where the Jacobian of  $f$ ,

$$J(x) = \nabla f(x), \quad (6)$$

was assumed to be nonsingular (invertible) with polar decomposition  $J = Qh$ ,  $Q = Q^{-T}$  is orthogonal,  $g = h^T h$  is the positive definite metric tensor,  $(\cdot)^T$  is the transpose,  $h$  is a positive definite matrix and

$$\tilde{\mathcal{V}}(x, t) = \mathcal{V}(f(x), t) \quad (7)$$

is the transformed potential.<sup>38</sup>

In this work, we derive necessary and sufficient conditions for the existence of an exact potential in a noise-driven system given by Eq. (2). After briefly recalling some of the special properties of potential systems driven by purely additive noise (PANs), we study their transformation rules under the mapping  $f$  from a continuum-mechanical perspective before applying our results to broadly studied examples of nonlinear oscillatory systems.

## II. NOISE-DRIVEN POTENTIAL FLOWS

### A. Special properties

In this section, we list a few of the simplifications, compared to general dynamical systems, which offer themselves for PANs. We first analyze the stochastic case with  $\Gamma \neq 0$  using the Fokker-Planck equation (FPE), which describes the evolution of the joint probability density function  $P: \mathbb{R}^n \rightarrow \mathbb{R}$  of a random dynamic variable  $x$  over time.<sup>1,2</sup> The FPE associated with the LP (1) reads

$$\frac{\partial P(x, t)}{\partial t} = \nabla \cdot \left[ P(x, t) \nabla \mathcal{V}(x, t) + \frac{\Gamma}{2} \nabla P(x, t) \right]. \quad (8)$$

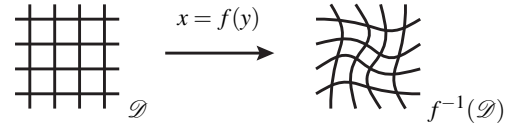


Figure 1. Cartesian coordinates  $x \in \mathcal{D}$  and their transformed counterparts  $y \in f^{-1}(\mathcal{D})$ , both represented in the  $x$ -frame. If potential systems driven by additive noise are described in transformed variables, the corresponding exact potentials can be identified through the systems' differential-geometric properties, which are studied in this work.

Assuming a steady potential  $\partial \mathcal{V} / \partial t = 0$ , we make the substitution

$$P(x, t) = G(x, t) \exp\left(\frac{-2\mathcal{V}(x)}{\Gamma}\right), \quad (9)$$

which leads to an advection–diffusion equation for  $G$ :

$$\frac{\partial G(x, t)}{\partial t} + v(x) \cdot \nabla G(x, t) = \frac{\Gamma}{2} \nabla^2 G(x, t), \quad (10)$$

where  $v(x) = -\nabla \mathcal{V}(x)$  is the velocity field of the gradient flow. Equation (10) is analytically solvable in special cases.<sup>39–41</sup> Of special interest is the exact solution of Eq. (10) given by  $G = \text{const.}$ , which corresponds to the stationary PDF  $P(x, t \rightarrow \infty) = P_\infty(x)$ :

$$P_\infty(x) = \mathcal{N} \exp\left(\frac{-2\mathcal{V}(x)}{\Gamma}\right), \quad (11)$$

where  $\mathcal{N} \in \mathbb{R}^+$  is a normalization constant. As shown below, the stationary PDF of the TLP (5) can be derived in analogous fashion:

$$\tilde{P}_\infty(x) = \mathcal{N} \exp\left(\frac{-2\tilde{\mathcal{V}}(x)}{\Gamma}\right). \quad (12)$$

In the deterministic limit  $\Gamma = 0$  and for time-varying potential, the TLP (5) is reduced to the transformed gradient system (TGS)

$$\dot{x} = -g^{-1}(x) \nabla \tilde{\mathcal{V}}(x, t). \quad (13)$$

Equation (13) states that trajectories  $x(t)$  are attracted to lower values of the potential  $\tilde{\mathcal{V}}$ , the attraction being equal to the potential gradient scaled with the inverse metric tensor  $g^{-1}$ . By definition and by the positive definiteness of  $g$ , any stationary potential  $\tilde{\mathcal{V}}$ ,  $\partial \tilde{\mathcal{V}} / \partial t = 0$ , is a Lyapunov function of the variables  $x$  evolving under Eq. (13) and thus determines the local and global stability of its trajectories.<sup>42</sup>

### B. Self-consistent modeling

Given a system of the form

$$\dot{x} = -\mathcal{M}(x) \nabla \tilde{\mathcal{V}}(x, t), \quad (14)$$

where  $\mathcal{M}$  is an arbitrary positive definite matrix, one can directly identify a TGS by defining  $g^{-1} = \mathcal{M}$ . Furthermore,

we recall that the Cholesky decomposition of a real positive definite matrix is, for each  $x$ , uniquely defined as

$$\mathcal{M}(x) = \mathcal{L}(x)\mathcal{L}^T(x), \quad (15)$$

where  $\mathcal{L}$  is a lower triangular matrix with positive diagonal entries.<sup>43</sup> (p. 441) Since the diagonal of a triangular matrix contains its eigenvalues,  $\mathcal{L}$  is also positive definite. Comparing Eq. (15) to the definition

$$g^{-1}(x) = h^{-1}(x)h^{-T}(x) \quad (16)$$

and setting  $h^{-1} = \mathcal{L}$ , one can define the following corresponding PAN:

$$\dot{x} = -\mathcal{M}(x)\nabla\tilde{\mathcal{V}}(x,t) + \mathcal{L}(x)\Xi, \quad (17)$$

where  $\Xi$  is a vector containing white noise sources of equal intensity. For a stationary potential  $\partial\mathcal{V}/\partial t = 0$ , under the above assumptions, the exact steady-state PDF of this system is given by Eq. (12).

### III. TRANSFORMATION RULES

#### A. Gradient flow

We now derive the transformation rules for PANs given by Eq. (1), beginning with the gradient term. We use the Einstein summation convention, by which repeated indices in a product imply summation over these indices. In index form, the LP (1) with  $\Xi = 0$  reads

$$\dot{x}_k = -\frac{d\mathcal{V}(x,t)}{dx_k}, \quad (18)$$

for  $k = 1, \dots, n$ , where the partial  $x$ -derivatives in  $\nabla$  have been rewritten as total derivatives because  $\mathcal{V}$  depends only on the (spatially) independent variables  $x$  and  $t$ . Under the transformation  $x = f(y)$ , suppressing for brevity the dependence of  $f$  on  $y$  in the argument of  $\mathcal{V}$ , Eq. (18) becomes

$$\begin{aligned} \frac{df_k(y)}{dy_i} \frac{dy_i}{dt} &= -\frac{dy_j}{dx_k} \frac{d\mathcal{V}(f,t)}{dy_j} \\ &= -\frac{dy_j}{df_k(y)} \frac{d\mathcal{V}(f,t)}{dy_j}, \end{aligned} \quad (19)$$

which can be rewritten as

$$\frac{dy_i}{dt} = -\frac{dy_i}{df_k(y)} \frac{dy_j}{df_k(y)} \frac{d\mathcal{V}(f,t)}{dy_j}. \quad (20)$$

The formula for the squared length of an infinitesimal line element  $ds^2$  in general curvilinear coordinates  $y$  is

$$ds^2 = g_{ij}dy_idy_j, \quad (21)$$

and the value of this quantity is independent of the coordinate system<sup>44</sup>. To relate  $ds^2$  to the original coordinates  $x$ , we consider the case where the mapping  $f$  is simply the identity:  $x = y$ . This gives  $g_{ij} = I_{ij}$ , where  $I$  is the identity matrix, so that

$$ds^2 = dx_k dx_k. \quad (22)$$

Multiplying both sides of Eq. (20) with  $g_{ij}$ , using Eq. (22) and noting that  $df_k = dx_k$ , we obtain

$$g_{ij} \frac{dy_i}{dt} = -\frac{d\mathcal{V}(f,t)}{dy_j}, \quad (23)$$

which can, by the symmetry of the metric tensor  $g$ , be written in vector form as follows:

$$\dot{y} = -g^{-1}(y)\nabla_y\tilde{\mathcal{V}}(y,t), \quad (24)$$

where  $(\nabla_y)_i = \partial/\partial y_i$  and the transformed potential was defined as  $\tilde{\mathcal{V}}(y,t) = \mathcal{V}(f(y),t)$ . As before, we interchanged partial and total derivatives in going from Eq. (23) to Eq. (24) because  $\tilde{\mathcal{V}}$  depends on  $y$  solely through  $f$ , and therefore the chain rule is the same for  $\partial\tilde{\mathcal{V}}/\partial y_j$  as for  $d\tilde{\mathcal{V}}/dy_j$ , i.e., the two terms coincide:

$$\frac{d\tilde{\mathcal{V}}(f,t)}{dy_j} = \frac{d\tilde{\mathcal{V}}(f,t)}{df} \frac{df(y)}{dy_j} \quad (25)$$

$$= \frac{\partial\tilde{\mathcal{V}}(f,t)}{\partial f} \frac{\partial f(y)}{\partial y_j}. \quad (26)$$

We then infer from Eq. (24) that under the mapping  $x = f(y)$ , the potential gradient transforms like

$$-\nabla\mathcal{V}(x,t) \rightarrow -g^{-1}(y)\nabla_y\tilde{\mathcal{V}}(y,t). \quad (27)$$

Redefining  $y \rightarrow x$  and  $\nabla_y \rightarrow \nabla$  in Eq. (24) yields Eq. (13).

#### B. Noise term

Having studied the transformation properties of the deterministic gradient flow, we now turn to the noise term  $\Xi$  in Eq. (1). Knowing from Eq. (19) that under the mapping  $x = f(y)$ ,  $\dot{x}_k = J_{kj}\dot{y}_j$ , where  $J_{kj} = \partial f_k/\partial y_j$ , we can infer that  $\Xi$  transforms like

$$\Xi \rightarrow J^{-1}(y)\Xi(\tilde{\Xi}). \quad (28)$$

The problem one now faces is that it is not clear a priori how  $\Xi$  is related to the transformed noise vector  $\tilde{\Xi}$  i.e., the noise vector in  $y$ -coordinates. To resolve this issue, we assume that  $\tilde{\Xi}$  preserves the noise intensity and the local orientation of  $\Xi$  in the original coordinates. In other words, for  $x \rightarrow f(y)$ ,  $\Xi$  behaves like an objective vector field transformed by an orthogonal tensor field  $Q = Q^{-T}$  representing the local rotation or reflection associated with  $f$ .<sup>45</sup>

$$\Xi = Q(y)\tilde{\Xi}. \quad (29)$$

Note that  $Q$  can be directly obtained from the polar decomposition of the Jacobian of  $f$ :

$$J(y) = Q(y)h(y), \quad (30)$$

where  $h$  is a positive definite matrix (since  $J$  is, by assumption, invertible) of the same size as  $J$  and  $Q$ .<sup>43</sup> (p. 449) Using Eqs. (29)-(30), the transformation formula (28) can be simplified as follows:

$$\Xi \rightarrow h^{-1}(y)\tilde{\Xi}. \quad (31)$$

Combining Eqs. (27) and (31) yields the TLP for systems with purely additive noise:

$$\dot{y} = -g^{-1}(y)\nabla_y \tilde{\mathcal{V}}(y,t) + h^{-1}(y)\tilde{\Xi}. \quad (32)$$

Redefining  $y \rightarrow x$ ,  $\nabla_y \rightarrow \nabla$  and  $\tilde{\Xi} \rightarrow \Xi$  reduces Eq. (32) to Eq. (5).

We stress that the assumptions made on the noise term in order to obtain Eq. (29) are not trivial, and that there may be situations where multiplicative noise terms appear that do not transform according to the same formula. Nevertheless, the special case described by Eq. (5) correctly identifies the exact potentials in the examples presented below.

### C. Fokker–Planck equation

The probability  $\mathcal{P}$  of the state  $x$  being inside the domain  $\mathcal{D}$  at time  $t$  is defined as

$$\mathcal{P} = \int_{\mathcal{D}} P(x,t) dV, \quad (33)$$

where  $dV = dx_1, \dots, dx_n$  is the volume element. In  $y$ -coordinates, using  $\det(J) = \det(h)$ , where  $\det$  is the determinant, Eq. (33) can be rewritten as

$$\mathcal{P} = \int_{\tilde{\mathcal{D}}} P(f(y),t) |\det(h(y))| d\tilde{V}, \quad (34)$$

where  $d\tilde{V} = dy_1, \dots, dy_n$  is the transformed volume element and  $\tilde{\mathcal{D}} = f^{-1}(\mathcal{D})$  is the transformed domain. We learn from Eq. (34) that the PDF  $P$  transforms like

$$P(x,t) \rightarrow |\det(h(y))| P(f(y),t) \quad (35)$$

under the mapping  $x = f(y)$ . Given a TLP (5), one can directly obtain  $\det(h)$  by computing the determinant of the matrix  $h^{-1}$  and using  $\det(h^{-1}) = \det(h)^{-1}$ . Typically, however, there is no interest in this geometric prefactor and the quantity of importance is the transformed PDF

$$\tilde{P}(y,t) = P(f(y),t). \quad (36)$$

Comparing Eq. (11) to Eq. (35), we observe that the steady-state solution  $P_{\infty}$  of the LP (1) with stationary potential transforms under  $f$  like

$$P_{\infty}(x) \rightarrow |\det(h(y))| \tilde{P}_{\infty}(y). \quad (37)$$

Knowledge of  $\tilde{\mathcal{V}}$  is sufficient to deduce the transformed stationary PDF

$$\tilde{P}_{\infty}(y) = \mathcal{N} \exp\left(\frac{-2\tilde{\mathcal{V}}(y)}{\Gamma}\right), \quad (38)$$

which, after redefining  $y \rightarrow x$ , coincides with Eq. (12).

## IV. POTENTIAL IDENTIFICATION

In the stochastic case, if  $\Xi$  is an additive noise vector with nonzero entries satisfying the assumptions made in the previous section and  $\mathcal{B}$  is nonsingular, identifying the exact potential  $\tilde{\mathcal{V}}$  of a general noise-driven system (2) is straightforward. By comparison with the TLP (5),  $h$  and  $g = h^T h$  are directly obtained from Eq. (2):

$$h(x) = \mathcal{B}^{-1}(x), \quad (39)$$

$$g(x) = \mathcal{B}^{-T}(x)\mathcal{B}^{-1}(x). \quad (40)$$

We recall that three-dimensional potential systems are uniquely defined by the vector identity

$$\text{curl grad}(\cdot) = 0, \quad (41)$$

i.e., the curl of a vector field is zero if and only if the vector field can be written as the gradient of a scalar function. Generalized to arbitrary dimensions, the equivalent identity reads

$$\text{skew}[\nabla^2(\cdot)] = 0, \quad (42)$$

where  $\text{skew}(\cdot)$  is the skew-symmetric part and  $\nabla^2(\cdot)$  is the Hessian matrix. By comparing Eqs. (2) and (5) and using  $h^T h = g$ , then, the following criteria are readily deduced:

- (I) A general noise-driven system described by Eq. (2) has an exact potential if and only if there exists a positive definite symmetric tensor field  $\mathcal{M}$  such that

$$\text{skew}(\nabla[\mathcal{M}^{-1}(x)\mathcal{F}(x)]) = 0.$$

- (II) For nonzero additive noise  $\Xi \neq 0$  satisfying the assumptions made in Sec. III B and nonsingular  $\mathcal{B}$ , a noise-driven system given by Eq. (2) has an exact potential if and only if

$$\text{skew}(\nabla[\mathcal{B}^{-T}(x)\mathcal{B}^{-1}(x)\mathcal{F}(x)]) = 0.$$

If either (I) or (II) are satisfied, the term in the square bracket is proportional to the potential gradient. If (I) is satisfied,  $\mathcal{M}$  is proportional to the inverse metric tensor  $g^{-1}$ . Note that in the purely deterministic case  $\Xi = 0$ , (II) does not apply because in this case,  $\mathcal{B}$  is ill-defined.

The general criterion (I) involves the solution of an underdetermined system of ordinary differential equations for a matrix  $\mathcal{M}$  whose entries are constrained by its symmetry and positive definiteness, and is impractical for manual analysis. In the future, this criterion may be simplified or solved with computer algebra. In practice, finite-dimensional gradient systems with  $\Xi = 0$  are identified by inspection of Eq. (2) under consideration of the general form of a TLP (5). Specific examples are discussed below.

## V. EXAMPLES

We now demonstrate our method on some of the examples mentioned in Sec. I. In certain cases, we visualize the identified potentials for different parameter values. A more in-depth

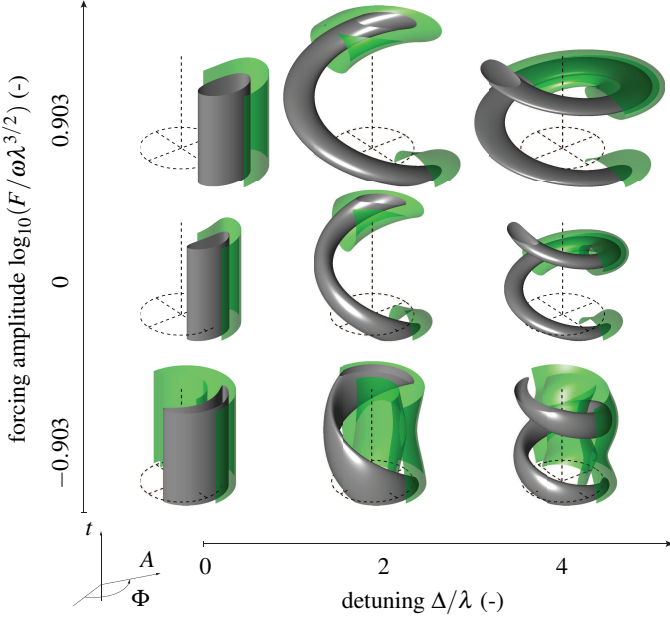


Figure 2. Illustration of the results derived in Sec. V A. Shown are isosurfaces of the time-dependent potential  $\tilde{\mathcal{V}}$  defined by Eq. (45) corresponding to 60% (green, one half shown) and 90% (gray) of its minimum value, as a function of the nondimensionalized forcing amplitude  $F/\omega\lambda^{3/2}$  and the detuning  $\Delta/\lambda$  (semi-log scale). Parameter values are given in the main text. The length of the dashed vertical line is  $2/\lambda$  and the dashed circle's radius is equal to the limit cycle amplitude  $2\sqrt{\lambda}$ .

analysis of these systems' nonlinear dynamics, which is out of the scope of this work, is left as a topic for future research. All equations are presented in the same form in which they appear in the references, up to minor changes in notation.

### A. Averaged Van der Pol oscillator

The weakly nonlinear dynamics of a harmonically forced, noise-driven Van der Pol oscillator synchronized with the forcing frequency  $\omega$  can be derived using deterministic and stochastic averaging. The resulting equations are<sup>17</sup> (Eqs. (7.58) and (7.59)<sup>46</sup>):

$$\dot{A} = \frac{A}{2} \left( \lambda - \frac{A^2}{4} \right) - \frac{F}{2\omega} \sin \varphi + \frac{\Gamma}{4A\omega^2} + \eta_1, \quad (43)$$

$$\dot{\varphi} = \Delta - \frac{F}{2\omega A} \cos \varphi + \frac{\eta_2}{A}, \quad (44)$$

where  $\Delta = (\omega_0^2 - \omega^2)/2\omega \approx \omega_0 - \omega$  is the detuning between the eigen- ( $\omega_0$ ) and the forcing ( $\omega$ ) frequency,  $2\sqrt{\lambda}$  is the limit cycle amplitude,  $F$  is the forcing amplitude,  $\Xi = (\eta_1, \eta_2)^T$  and  $\eta_{1,2}$  are uncorrelated white noise sources of equal intensity  $\Gamma/2\omega^2$ . Defining the new variables  $x = (A, \Phi)^T$ , where  $\Phi = \varphi - \Delta t$ , by criterion (II), Eqs. (43)-(44) have the form of a

TLP with  $g(x) = \text{diag}(1, A^2)$ ,  $h(x) = \text{diag}(1, A)$  and

$$\tilde{\mathcal{V}}(x, t) = -\frac{A^2\lambda}{4} + \frac{A^4}{32} + \frac{AF}{2\omega} \sin(\Phi + \Delta t) - \frac{\Gamma}{4\omega^2} \ln A. \quad (45)$$

The potential given by Eq. (45) is visualized in Fig. 2 for  $t \in [0, 2/\lambda]$ ,  $\omega = 5.03 \times 10^3$ ,  $\lambda$  equal to 2% of  $\omega$  and  $\Gamma = \lambda^2\omega^2/10$  (arbitrary units). We observe a double-layered structure of the potential which is more pronounced at small values of  $F/\omega\lambda^{3/2}$ , consistent with the notion that the (perturbed) self-sustained oscillation coexists with the forced response at small forcing amplitudes.<sup>17</sup> (pp. 180–190) We also note that at large forcing amplitudes, for nonzero detuning, the potential varies periodically in time, leading to beating oscillations, i.e., oscillations of the slow variables  $A$  and  $\varphi$ .<sup>17</sup> (pp. 174–177)

### B. Generalized Kuramoto model

A set of swarming oscillators (“swarmalators”) has been described by a generalized Kuramoto model:<sup>20</sup>

$$\dot{y}_i = \omega_i + \frac{\mathcal{J}}{N} \sum_j \sin(y_j - y_i) \cos(\theta_j - \theta_i), \quad (46)$$

$$\dot{\theta}_i = \omega_i + \frac{\mathcal{K}}{N} \sum_j \cos(y_j - y_i) \sin(\theta_j - \theta_i), \quad (47)$$

where  $i = 1, \dots, N$ ,  $n = 2N$  is the system dimension, the parameters  $\mathcal{J}, \mathcal{K} \in \mathbb{R}$  are coupling constants and  $v_i, \omega_i \in \mathbb{R}$  are the eigenfrequencies of the dynamic variables  $y_i$  and  $\theta_i$ . To observe the exact potential, we define the new variables  $x = (Y_1, \dots, Y_N, \Theta_1, \dots, \Theta_N)^T$ , where  $Y_i = y_i/\mathcal{J}$  and  $\Theta_i = \theta_i/\mathcal{K}$ . For  $\mathcal{J}, \mathcal{K} > 0$ , the resulting system is a TGS with  $g = \text{diag}(\mathcal{J}, \dots, \mathcal{J}, \mathcal{K}, \dots, \mathcal{K}) \in \mathbb{R}^n$  and

$$\tilde{\mathcal{V}}(x) = -\sum_k \left[ \frac{1}{2N} \sum_j \cos \mathcal{J}(Y_j - Y_k) \cos \mathcal{K}(\Theta_j - \Theta_k) + v_k Y_k + \omega_k \Theta_k \right]. \quad (48)$$

For  $N = 2$  and  $v_i = v$  and  $\omega_i = \omega$  for  $i = 1, 2$ , Eqs. (46) and (47) are equivalent to the following system describing the dynamics of the differences  $\Delta y = y_2 - y_1$  and  $\Delta \theta = \theta_2 - \theta_1$ <sup>20</sup> (Eqs. (76) and (77)<sup>47</sup>):

$$\Delta \dot{y} = -\mathcal{J} \sin \Delta y \cos \Delta \theta, \quad (49)$$

$$\Delta \dot{\theta} = -\mathcal{K} \sin \Delta \theta \cos \Delta y. \quad (50)$$

Analogous to the general case above, we define the new variables  $\Delta x = (\Delta Y, \Delta \Theta)^T$ ,  $\Delta Y = Y_2 - Y_1$  and  $\Delta \Theta = \Theta_2 - \Theta_1$  satisfying  $\Delta \dot{x} = -g^{-1} \nabla \mathcal{V}$  with

$$\tilde{\mathcal{V}}(x) = -\frac{1 + \cos(\mathcal{J} \Delta Y) \cos(\mathcal{K} \Delta \Theta)}{2} \quad (51)$$

and the metric tensor  $g = \text{diag}(\mathcal{J}, \mathcal{K})$ . It is worth noting that the system (49) and (50) is known to possess an exact

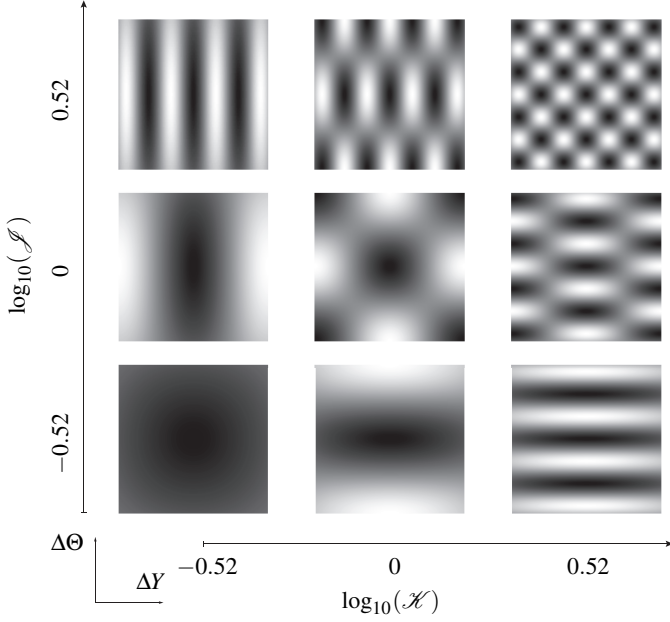


Figure 3. Illustration of the results derived in Sec. VB. Shown is the potential  $\mathcal{V}$  given by Eq. (51) over the periodic domain  $\Delta Y, \Delta\Theta \in [-\pi, \pi]$  for different values of the coupling constants  $\mathcal{J}$  and  $\mathcal{K}$  (logarithmic scale). The potential level is indicated in grayscale, ranging from black (attractive,  $\mathcal{V} = -1$ ) to white (repelling,  $\mathcal{V} = 0$ ).

limit cycle.<sup>20</sup> (pp. 7–8) This solution is not in contradiction to the well-known theorem on nonexistence of periodic orbits in autonomous gradient systems,<sup>48</sup> (p. 49) as it exists only for negative values of  $\mathcal{K}$ , for which the metric tensor defined above loses its positive definiteness and the assumptions of our method break down.

The potential (51) is visualized for different values of the coupling constants  $\mathcal{J}, \mathcal{K}$  in Fig. 3. We see that the synchronized state  $\Delta Y = \Delta\Theta = 0$  is always a potential minimum and therefore linearly stable for  $\mathcal{J}, \mathcal{K} > 0$ , which is consistent with an earlier stability analysis on the full system (46) and (47).<sup>20</sup> (pp. 4–5)

### C. Classical time crystal

The dynamics of a classical many-body time crystal have recently been studied,<sup>21</sup> leading to a system of even dimension  $n = 2N$  with linear dynamics

$$\dot{z} = \begin{pmatrix} a & b & b & \dots \\ b & a & b & \\ b & b & a & \\ \vdots & & & \ddots \end{pmatrix} z = Az. \quad (52)$$

The sub-matrices  $a, b \in \mathbb{R}^{2 \times 2}$  are

$$a = \begin{pmatrix} -\frac{\gamma}{2} & -\frac{\lambda\omega_0^2 + 2(\omega_0^2 - \omega^2)}{4\omega} \\ -\frac{\lambda\omega_0^2 + 2(\omega_0^2 - \omega^2)}{4\omega} & -\frac{\gamma}{2} \end{pmatrix},$$

$$b = \begin{pmatrix} 0 & \frac{\beta^2}{2\omega N} \\ -\frac{\beta^2}{2\omega N} & 0 \end{pmatrix},$$

where  $\gamma$  is the dissipation,  $\lambda$  is the parametric driving strength,  $\omega_0$  is the eigen- and  $2\omega$  is the parametric driving frequency. For simplicity, we consider a 4-by-4 block of Eq. (52) with variables  $z = (z_1, z_2, z_3, z_4)^T$ ,  $N = 2$  and

$$A = \begin{pmatrix} a & b \\ b & a \end{pmatrix}. \quad (53)$$

The non-symmetric matrices populating the anti-diagonal of  $A$  indicate the presence of reactive coupling which obstructs the direct identification of the potential. To circumvent this issue, we first make a transformation  $z = f(y)$  to amplitude-phase coordinates  $y = (A_1, A_2, \varphi_1, \varphi_2)^T$ :

$$z = \begin{pmatrix} A_1 \cos \varphi_1 \\ A_2 \cos \varphi_2 \\ A_2 \sin \varphi_2 \\ A_1 \sin \varphi_1 \end{pmatrix}. \quad (54)$$

The dynamics of the  $y$ -coordinates equivalent to Eq. (52) are

$$\dot{y} = \begin{pmatrix} -\frac{\gamma A_1}{2} - \frac{\lambda\omega_0^2 + 2(\omega_0^2 - \omega^2)}{4\omega} A_2 \cos(\varphi_1 - \varphi_2) \\ -\frac{\gamma A_2}{2} - \frac{\lambda\omega_0^2 + 2(\omega_0^2 - \omega^2)}{4\omega} A_1 \cos(\varphi_1 - \varphi_2) \\ -\frac{\beta^2}{4\omega} + \frac{\lambda\omega_0^2 + 2(\omega_0^2 - \omega^2)}{4\omega} \frac{A_2}{A_1} \sin(\varphi_1 - \varphi_2) \\ \frac{\beta^2}{4\omega} - \frac{\lambda\omega_0^2 + 2(\omega_0^2 - \omega^2)}{4\omega} \frac{A_1}{A_2} \sin(\varphi_1 - \varphi_2) \end{pmatrix},$$

which, defining the new variables  $x = (A_1, A_2, \Phi_1, \Phi_2)^T$  with  $\Phi_{1,2} = \varphi_{1,2} \pm \beta^2 t / 4\omega$ , corresponds to a TGS with  $g(x) = \text{diag}(1, 1, A_1^2, A_2^2)$  and

$$\tilde{\mathcal{V}}(x, t) = \frac{\gamma(A_1^2 + A_2^2)}{4} + \frac{\lambda\omega_0^2 + 2(\omega_0^2 - \omega^2)}{4\omega} A_1 A_2 \cos(\Phi_1 - \Phi_2 - \frac{\beta^2 t}{2\omega}). \quad (55)$$

### D. Coupled limit cycles

The weakly nonlinear amplitude-phase dynamics of two linearly coupled Van der Pol oscillators, derived using deter-

ministic averaging, are given by<sup>17</sup> (Eq. (4.11))

$$\dot{A}_1 = \frac{\lambda_1}{2}A_1 - \frac{1}{8}A_1^3 + \frac{C}{2}(A_2 \cos \phi - A_1), \quad (56)$$

$$\dot{A}_2 = \frac{\lambda_2}{2}A_2 - \frac{1}{8}A_2^3 + \frac{C}{2}(A_1 \cos \phi - A_2), \quad (57)$$

$$\dot{\phi} = \Delta - \frac{C}{2} \sin \phi \left( \frac{A_2}{A_1} + \frac{A_1}{A_2} \right), \quad (58)$$

where  $C$  is the coupling,  $\phi = \varphi_2 - \varphi_1$  is the phase difference and  $\Delta = (\omega_2^2 - \omega_1^2)/2\omega \approx \omega_2 - \omega_1$  is the detuning between the eigenfrequencies  $\omega_{1,2}$  and  $\omega$  is the frequency of the synchronized coupled oscillators  $\omega \approx \omega_{1,2}$ . If we define  $x = (A_1, A_2, \Phi)^T$ ,  $\Phi = \phi - \Delta t$ , then Eqs. (56)-(58) are equivalent a TGS with  $g^{-1}(x) = \text{diag}(1, 1, A_1^{-2} + A_2^{-2})$  and

$$\begin{aligned} \tilde{\mathcal{V}}(x, t) = & -\frac{\lambda_1 A_1^2 + \lambda_2 A_2^2}{4} + \frac{A_1^4 + A_2^4}{32} \\ & + \frac{C}{4} [A_1^2 + A_2^2 - 2A_1 A_2 \cos(\Phi + \Delta t)]. \end{aligned} \quad (59)$$

It is an open question whether the above results can simplify the stability analysis of Eqs. (56)-(58).<sup>17,22</sup> (pp. 81–84)

### E. Nonlinear coupling

The following set of nonlinearly coupled amplitude and phase equations are obtained by averaging the equation describing the projection of turbulence-driven thermoacoustic dynamics onto two orthogonal modes in an annular cavity<sup>24</sup> (see Fig. 4, left inset for a sketch of such a cavity):

$$\begin{aligned} \dot{A} = & \nu A - \frac{3\kappa}{32}(3A^2 + [2 + \cos(2\phi)]B^2)A \\ & + \frac{\Gamma}{4\omega_0^2 A} + \zeta_a, \end{aligned} \quad (60)$$

$$\begin{aligned} \dot{B} = & \nu B - \frac{3\kappa}{32}(3B^2 + [2 + \cos(2\phi)]A^2)B \\ & + \frac{\Gamma}{4\omega_0^2 B} + \zeta_b, \end{aligned} \quad (61)$$

$$\dot{\phi} = \frac{3\kappa(A^2 + B^2)}{32} \sin(2\phi) + \left( \frac{1}{A} + \frac{1}{B} \right) \zeta_\phi, \quad (62)$$

where  $A$  and  $B$  are the amplitudes,  $\phi = \varphi_a - \varphi_b$  is the phase difference,  $\omega_0$  is the eigenfrequency,  $\nu$  is the growth rate,  $\kappa$  is the nonlinearity constant,  $\Xi = (\zeta_a, \zeta_b, \zeta_\phi)^T$  and  $\zeta_a, \zeta_b, \zeta_\phi$  are white noise sources of equal intensity  $\Gamma/2\omega_0^2$ . Equation (62) can be rewritten as two separate equations for the phases  $\varphi_a$  and  $\varphi_b$ :

$$\dot{\varphi}_a = \frac{3\kappa B^2}{32} \sin 2(\varphi_a - \varphi_b) + \frac{\xi_a}{A}, \quad (63)$$

$$\dot{\varphi}_b = -\frac{3\kappa A^2}{32} \sin 2(\varphi_a - \varphi_b) + \frac{\xi_b}{B}, \quad (64)$$

where  $\xi_{a,b}$  are white noise sources of intensity  $\Gamma/2\omega_0^2$ . Starting from Eqs. (63)-(64), Eq. (62) can be derived by taking the difference between the former two equations and

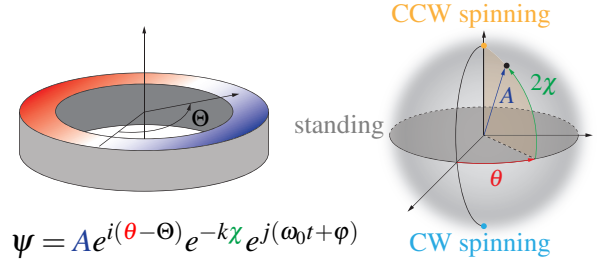


Figure 4. Illustration of the examples presented in Sec. VE and VF. In this representation, a self-oscillating mode  $\psi$  in an annular cavity is projected onto four variables  $x = (A, \theta, \chi, \varphi)^T$  using the basic quaternions  $(i, j, k)$  (left inset).<sup>25–27,49</sup> Different states such as pure spinning and standing waves are mapped to different points on the Bloch sphere (right inset). The same coordinate system is used to represent the PDF isosurfaces in Fig. 5.

setting  $\xi_a = -\xi_b = \zeta_\phi$ . According to criterion (II), Eqs. (60), (61), (63) and (64) correspond to a TLP with  $x = (A, B, \varphi_a, \varphi_b)^T$ ,  $\Xi = (\zeta_a, \zeta_b, \xi_a, \xi_b)^T$ ,  $g(x) = \text{diag}(1, 1, A^2, B^2)$ ,  $h(x) = \text{diag}(1, 1, A, B)$  and

$$\begin{aligned} \tilde{\mathcal{V}}(x) = & -\frac{\nu(A^2 + B^2)}{2} + \frac{3\kappa}{128}(3(A^4 + B^4) \\ & + 2A^2 B^2 [2 + \cos 2(\varphi_a - \varphi_b)]) \\ & - \frac{\Gamma}{4\omega_0^2} \ln(AB). \end{aligned} \quad (65)$$

### F. Quaternion flow

In the study of self-oscillating thermoacoustic modes in annular cavities, an alternative projection to the one used in the previous example and based on the quaternion Fourier transform for bivariate signals<sup>50</sup> offers a convenient description of the nature of the modal dynamics, where one of the state variables indicates whether spinning or standing waves govern the dynamics at a given time instant.<sup>25–27,49</sup> Indeed, by projecting the acoustic field  $\psi(\Theta, t)$  depending on the azimuthal angle  $\Theta$  onto the four state variables  $x = (A, \chi, \theta, \varphi)^T$  using the basic quaternions  $(i, j, k)$ , the instantaneous state can be mapped to different points on the Bloch sphere.<sup>49</sup> In this representation, counter-clockwise (CCW) and clockwise (CW) spinning waves correspond to the north ( $2\chi = \pi/2$ ) and south ( $2\chi = -\pi/2$ ) poles, while the equatorial plane ( $\chi = 0$ ) describes pure standing waves (Fig. 4). In general, the system state is a mixture between a standing and a spinning wave. The variable  $\theta$  describes the orientation of the nodal line of the standing wave component of  $\psi$ . By deterministic and stochastic averaging of the projected acoustic wave equation, the following dynamics for  $x$  can be derived:<sup>25</sup> (pp. 20–23)

$$\dot{x} = \mathcal{F}(x) + \mathcal{B}(x)\Xi. \quad (66)$$

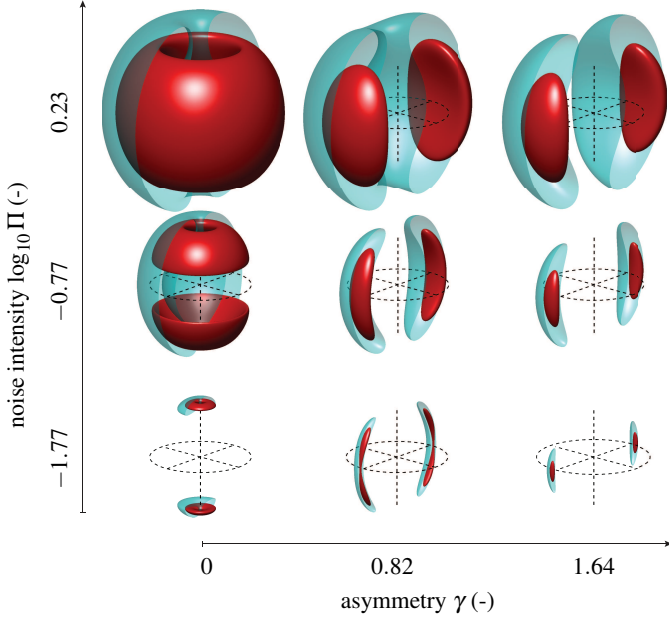


Figure 5. Illustration of the results derived in Secs. V F. Shown are isosurfaces of the transformed stationary PDF  $\tilde{P}_\infty$  given by Eqs. (12) and (72) corresponding to 25% (red) and 75% (cyan, one half shown) of its maximum value, as a function of the nondimensionalized noise intensity  $\Pi$  and asymmetry  $\gamma$  (semi-log scale, definitions in the main text). The spherical coordinate system used to represent the PDF is defined in Fig. 4. The length of the dashed vertical line and the dashed circle's radius are both equal to  $8\sqrt{v/15\kappa}$ . The spatial structure of the analytical Fokker–Planck solution shown in this figure is in excellent agreement with corresponding numerical simulations.<sup>27</sup> (Fig. 11)

The entries of the deterministic term  $\mathcal{F}$  in Eq. (66) are

$$\mathcal{F}_1 = \left( v + \frac{c}{4} \cos(2\theta) \cos(2\chi) \right) A - \frac{3\kappa}{64} [5 + \cos(4\chi)] A^3 + \frac{3\Gamma}{4\omega_0^2 A}, \quad (67)$$

$$\mathcal{F}_2 = \frac{3\kappa}{64} A^2 \sin(4\chi) - \frac{c}{4} \cos(2\theta) \sin(2\chi) - \frac{\Gamma \tan(2\chi)}{2\omega_0^2 A^2}, \quad (68)$$

$$\mathcal{F}_3 = -\frac{c \sin(2\theta)}{4 \cos(2\chi)}, \quad (69)$$

$$\mathcal{F}_4 = \frac{c}{4} \sin(2\theta) \tan(2\chi), \quad (70)$$

where  $v$  is the growth rate,  $\kappa$  is the nonlinearity constant,  $\omega_0$  is the eigenfrequency and  $c$  is the asymmetry. The entries of the noise vector  $\Xi = (\zeta_A, \zeta_\chi, \zeta_\theta, \zeta_\varphi)^T$  each have equal intensity  $\Gamma/2\omega_0^2$  and the matrix  $\mathcal{B}$  describing the stochastic coupling is

given in the reference as<sup>51</sup>

$$\mathcal{B} = \begin{pmatrix} 1 & 0 & 0 & 0 \\ 0 & A^{-1} & 0 & 0 \\ 0 & 0 & \frac{1}{A \cos 2\chi} & 0 \\ 0 & 0 & -\frac{\tan 2\chi}{A} & A^{-1} \end{pmatrix}. \quad (71)$$

By criterion (II), Eqs. (66)-(71) describe a TLP with

$$g^{-1}(x) = \begin{pmatrix} 1 & 0 & 0 & 0 \\ 0 & A^{-2} & 0 & 0 \\ 0 & 0 & \frac{1}{A^2 \cos(2\chi)^2} & -\frac{\tan 2\chi}{A^2 \cos 2\chi} \\ 0 & 0 & -\frac{\tan 2\chi}{A^2 \cos 2\chi} & A^{-2} + \frac{\tan(2\chi)^2}{A^2} \end{pmatrix},$$

$$h^{-1}(x) = \mathcal{B}(x),$$

and the transformed potential

$$\begin{aligned} \tilde{\mathcal{V}}(x) = & - \left( v + \frac{c}{4} \cos(2\theta) \cos(2\chi) \right) \frac{A^2}{2} \\ & + \frac{3\kappa}{256} [5 + \cos(4\chi)] A^4 \\ & - \frac{3\Gamma}{4\omega_0^2} \ln(A) - \frac{\Gamma}{4\omega_0^2} \ln(\cos(2\chi)). \end{aligned} \quad (72)$$

In Fig. 5, we plot the transformed stationary PDF  $\tilde{P}_\infty(x)$  given by Eqs. (12) and (72) in the spherical coordinate system  $(A, 2\chi, \theta)$  on a semi-log scale for different values of the nondimensionalized noise intensity  $\Pi$  and asymmetry  $\gamma$ :

$$\Pi = \frac{27\kappa\Gamma}{256v^2\omega_0^2}, \quad (73)$$

$$\gamma = \frac{c}{2v}. \quad (74)$$

As  $\gamma$  is increased from zero, a preferred direction in  $\theta$  emerges in the steady state, demonstrating the explicitly broken symmetry of the system for  $\gamma \neq 0$ . The spatial structure of the analytical PDF  $\tilde{P}_\infty$  shown in Fig. 5 is in excellent agreement with numerical simulations of the Fokker–Planck equation for the same parameter values.<sup>27</sup> (Fig. 11)

## VI. CONCLUSIONS

In this study, we derived necessary and sufficient criteria for the existence of an exact potential in a general noise-driven system. We demonstrated on several broadly studied models of deterministic and stochastic oscillations that from the differential-geometric properties of transformed potential systems driven by additive noise, one can derive new analytical descriptions of their nonlinear dynamics. Systems to which this method applies appear to be ubiquitous and are often found in the context of time-averaged flows. The question of *why* this is the case is left for future research to answer.



We demonstrated our method on several examples, and so obtained new analytical descriptions of beating, synchronization and symmetry breaking.

To conclude, we mention that our theoretical approach implies a self-consistent way of modeling noise in given deterministic gradient flows, and that the resulting models are exactly solvable if the potential is stationary.

## ACKNOWLEDGEMENTS

The authors acknowledge helpful discussions with Kevin O’Keeffe about his previous work on swarming oscillators. This project is funded by the Swiss National Science Foundation under Grant agreement 184617.

## AUTHOR DECLARATIONS

### Conflict of Interest

The authors have no conflicts to disclose.

## DATA AVAILABILITY

The datasets used for generating the plots in this study can be directly obtained by numerical simulation of the related mathematical equations in the manuscript.

## REFERENCES

- <sup>1</sup>C. W. Gardiner *et al.*, *Handbook of stochastic methods*, Vol. 4 (Springer Berlin, 1985).
- <sup>2</sup>H. Risken, *The Fokker-Planck Equation* (Springer, 1984) pp. 63–95.
- <sup>3</sup>R. Stratonovich, *Topics in the Theory of Random Noise Vol. I: General Theory of Random Processes Nonlinear Transformations of Signals and Noise* (Gordon & Breach, 1963).
- <sup>4</sup>P. Hänggi and F. Marchesoni, “Introduction: 100 years of Brownian motion,” *Chaos* **15** (2005).
- <sup>5</sup>M. Zaks, X. Sailer, L. Schimansky-Geier, and A. Neiman, “Noise induced complexity: From subthreshold oscillations to spiking in coupled excitable systems,” *Chaos* **15** (2005).
- <sup>6</sup>H. Nakao, J.-N. Teramae, D. Goldobin, and Y. Kuramoto, “Effective long-time phase dynamics of limit-cycle oscillators driven by weak colored noise,” *Chaos* **20** (2010).
- <sup>7</sup>R. Yamapi, G. Filatrella, M. Aziz-Alaoui, and H. Cerdeira, “Effective Fokker–planck equation for birhythmic modified Van der Pol oscillator,” *Chaos* **22** (2012).
- <sup>8</sup>A. Frishman and P. Ronceray, “Learning force fields from stochastic trajectories,” *Phys. Rev. X* **10** (2020).
- <sup>9</sup>M. Santos Gutiérrez, V. Lucarini, M. Chekroun, and M. Ghil, “Reduced-order models for coupled dynamical systems: Data-driven methods and the Koopman operator,” *Chaos* **31** (2021).
- <sup>10</sup>J. Stuart, “On the non-linear mechanics of hydrodynamic stability,” *J. Fluid Mech.* **4** (1958).
- <sup>11</sup>L. D. Landau and E. M. Lifshitz, *Fluid mechanics*, Vol. 11 (Pergamon Press Oxford, UK, 1959).
- <sup>12</sup>M. Lax, “Classical noise. v. noise in self-sustained oscillators,” *Phys. Rev.* **160**, 290–307 (1967).
- <sup>13</sup>V. I. Arnold, *Geometrical methods in the theory of ordinary differential equations*, Vol. 250 (Springer Science & Business Media, 2012).
- <sup>14</sup>B. Van der Pol, “LXXXVIII. on “relaxation-oscillations,”” *London Edinburgh Philos. Mag. J. Sci.* **2**, 978–992 (1926).
- <sup>15</sup>J. A. Sanders, F. Verhulst, and J. Murdock, *Averaging methods in nonlinear dynamical systems*, Vol. 59 (Springer, 2007).
- <sup>16</sup>J. Roberts and P. Spanos, “Stochastic averaging: An approximate method of solving random vibration problems,” *Int. J. Non-Linear Mech.* **21**, 111–134 (1986).
- <sup>17</sup>A. Balanov, N. Janson, D. Postnov, and O. Sosnovtseva, *From simple to complex* (Springer, 2009).
- <sup>18</sup>Y. Kuramoto, “Chemical turbulence,” in *Chemical oscillations, waves, and turbulence* (Springer, 1984) pp. 111–140.
- <sup>19</sup>S. Strogatz, “From kuramoto to crawford: Exploring the onset of synchronization in populations of coupled oscillators,” *Physica D* **143**, 1–20 (2000).
- <sup>20</sup>K. O’Keeffe, S. Ceron, and K. Petersen, “Collective behavior of swarmalators on a ring,” *Phys. Rev. E* **105** (2022).
- <sup>21</sup>T. L. Heugel, M. Oscity, A. Eichler, O. Zilberberg, and R. Chitra, “Classical many-body time crystals,” *Phys. Rev. Lett.* **123** (2019).
- <sup>22</sup>D. Aronson, G. Ermentrout, and N. Kopell, “Amplitude response of coupled oscillators,” *Physica D* **41** (1990).
- <sup>23</sup>T. Pedergnana and N. Noiray, “Steady-state statistics, emergent patterns and intermittent energy transfer in a ring of oscillators,” *Nonlinear Dyn.* **108** (2022).
- <sup>24</sup>N. Noiray and B. Schuermans, “On the dynamic nature of azimuthal thermoacoustic modes in annular gas turbine combustion chambers,” *Proc. R. Soc. A* **469** (2013).
- <sup>25</sup>A. Faure-Beaulieu and N. Noiray, “Symmetry breaking of azimuthal waves: Slow-flow dynamics on the bloch sphere,” *Phys. Rev. Fluids* **5** (2020).
- <sup>26</sup>G. Ghirardo and F. Gant, “Averaging of thermoacoustic azimuthal instabilities,” *J. Sound Vib.* **490** (2021).
- <sup>27</sup>T. Indlekofer, A. Faure-Beaulieu, J. R. Dawson, and N. Noiray, “Spontaneous and explicit symmetry breaking of thermoacoustic eigenmodes in imperfect annular geometries,” *J. Fluid Mech.* **944**, A15 (2022).
- <sup>28</sup>G. Rigas, A. Morgans, R. Brackston, and J. Morrison, “Diffusive dynamics and stochastic models of turbulent axisymmetric wakes,” *J. Fluid Mech.* **778** (2015).
- <sup>29</sup>M. Sieber, C. Paschereit, and K. Oberleithner, “Stochastic modelling of a noise-driven global instability in a turbulent swirling jet,” *J. Fluid Mech.* **916** (2021).
- <sup>30</sup>J. Tchoufag, D. Fabre, and J. Magnaudet, “Weakly nonlinear model with exact coefficients for the fluttering and spiraling motion of buoyancy-driven bodies,” *Phys. Rev. Lett.* **115** (2015).
- <sup>31</sup>R. Graham and T. Tél, “Steady-state ensemble for the complex ginzburg-landau equation with weak noise,” *Phys. Rev. A* **42**, 4661–4677 (1990).
- <sup>32</sup>R. Graham and T. Tél, “Nonequilibrium potentials in spatially extended pattern forming systems,” in *Instabilities and Nonequilibrium Structures III*, edited by E. Tirapegui and W. Zeller (Springer Netherlands, Dordrecht, 1991) pp. 125–142.
- <sup>33</sup>O. Descalzi and R. Graham, “Nonequilibrium potential for the ginzburg-landau equation in the phase-turbulent regime,” *Z. Phys. B* **93**, 509–513 (1994).
- <sup>34</sup>R. Montagne, E. Hernández-García, and M. San Miguel, “Numerical study of a lyapunov functional for the complex ginzburg-landau equation,” *Physica D* **96**, 47–65 (1996).
- <sup>35</sup>G. Izús, R. Deza, and H. Wio, “Exact nonequilibrium potential for the fitzhugh-nagumo model in the excitable and bistable regimes,” *Phys. Rev. E* **58**, 93–98 (1998).
- <sup>36</sup>J. Zhou, D. Aliyu, E. Aurell, and S. Huang, “Quasi-potential landscape in complex multi-stable systems,” *J. R. Soc. Interface* **9**, 3539–3553 (2012).
- <sup>37</sup>M. Cameron, “Finding the quasipotential for nongradient sdes,” *Physica D* **241**, 1532–1550 (2012).
- <sup>38</sup>Unless explicitly stated otherwise, all quantities in this work are assumed to be real.
- <sup>39</sup>J. Philip, “Some exact solutions of convection-diffusion and diffusion equations,” *Water Resour. Res.* **30** (1994).
- <sup>40</sup>C. Zoppou and J. Knight, “Analytical solutions for advection and advection-diffusion equations with spatially variable coefficients,” *J. Hydraul. Eng.* **123** (1997).
- <sup>41</sup>C. Zoppou and J. Knight, “Analytical solution of a spatially variable coefficient advection-diffusion equation in up to three dimensions,” *Appl. Math. Model.* **23** (1999).

- <sup>42</sup>A. Lyapunov, “The general problem of the stability of motion,” *Int. J. Control* **55**, 531–534 (1992).
- <sup>43</sup>R. A. Horn and C. R. Johnson, *Matrix analysis* (Cambridge University press, 2012).
- <sup>44</sup>W. Kühnel, *Differential geometry*, Vol. 77 (American Mathematical Society, 2015).
- <sup>45</sup>C. Truesdell and W. Noll, “The non-linear field theories of mechanics,” in *The non-linear field theories of mechanics* (Springer, 2004) pp. 1–579.
- <sup>46</sup>Due to a typographical error, the “ $A^2$ ” in the bracket is missing in Eq. (7.58) of the reference.
- <sup>47</sup>Due to a typographical error, the minus signs are missing in Eqs. (76) and (77) of the reference.
- <sup>48</sup>J. Guckenheimer and P. Holmes, *Nonlinear oscillations, dynamical systems, and bifurcations of vector fields*, Vol. 42 (Springer Science & Business Media, 2013).
- <sup>49</sup>G. Ghirardo and M. Bothien, “Quaternion structure of azimuthal instabilities,” *Phys. Rev. Fluids* **3** (2018).
- <sup>50</sup>J. Flamant, N. Le Bihan, and P. Chainais, “Time–frequency analysis of bivariate signals,” *Appl. Comput. Harmon. Anal.* **46**, 351–383 (2017).
- <sup>51</sup>Due to a typographical error, the matrix defined in Eq. (78) of the reference should instead be equal to its transpose.